

AD-761 825

CONSIDERATIONS IN SHIELDING ANALYSIS OF
JOINTS AND CONNECTORS IN CABLE SYSTEMS

STANFORD RESEARCH INSTITUTE

PREPARED FOR
AIR FORCE WEAPONS LABORATORY

MAY 1973

Distributed By:

NTIS

National Technical Information Service
U. S. DEPARTMENT OF COMMERCE

AD 761825



CONSIDERATIONS IN SHIELDING ANALYSIS OF JOINTS AND CONNECTORS IN CABLE SYSTEMS

S. Dairiki

Stanford Research Institute

TECHNICAL REPORT NO. AFWL-TR-73-73

May 1973

AIR FORCE WEAPONS LABORATORY

Air Force System Command

Kirtland Air Force Base

New Mexico

Reproduced by
NATIONAL TECHNICAL
INFORMATION SERVICE
U.S. Department of Commerce
Springfield VA 22151



Approved for public release; distribution unlimited.

64

AIR FORCE SPECIAL WEAPONS CENTER
 Air Force Systems Command
 Kirtland Air Force Base
 New Mexico 87117

ACQUISITION IN	
MTIS	WHIP Section <input checked="" type="checkbox"/>
DTC	WHIP Section <input type="checkbox"/>
UNCLASSIFIED	<input type="checkbox"/>
ACQUISITION	
BY	
UNCLASSIFIED ACQUISITION CODES	
DIS. ACQUISITION SPECIAL	
A	

When US Government drawings, specifications, or other data are used for any purpose other than a definitely related Government procurement operation, the Government thereby incurs no responsibility nor any obligation whatsoever, and the fact that the Government may have formulated, furnished, or in any way supplied the said drawings, specifications, or other data, is not to be regarded by implication or otherwise, as in any manner licensing the holder or any other person or corporation, or conveying any rights or permission to manufacture, use, or sell any patented invention that may in any way be related thereto.

DO NOT RETURN THIS COPY. RETAIN OR DESTROY.

AFWL-TR-73-73

CONSIDERATIONS IN SHIELDING ANALYSIS OF JOINTS
AND CONNECTORS IN CABLE SYSTEMS

S. Dairiki
Stanford Research Institute

TECHNICAL REPORT NO. AFWL-TR-73-73

Approved for public release; distribution unlimited.

FOREWORD

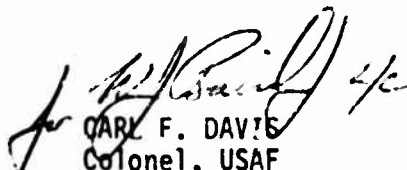
This report was prepared by the Stanford Research Institute, Menlo Park, California, under Contract F29601-69-C-0127. The research was performed under Program Element 11213F, Project 133B, and was funded by the Space and Missile Systems Organization (SAMSO).

Inclusive dates of research were July 1971 through February 1972. The report was submitted 21 March 1973 by the Air Force Weapons Laboratory Project Officer, Captain Wayne D. Wilson (ELE).

This technical report has been reviewed and is approved.


WAYNE D. WILSON
Captain, USAF
Project Officer


JOHN F. PORTASIK
Colonel, USAF
Chief, Electromagnetic Pulse Branch


CARL F. DAVIS
Colonel, USAF
Chief, Electronics Division

CONTENTS

I	INTRODUCTION	1
II	APERTURE LEAKAGE AND EQUIVALENT SOURCES	5
	A. Aperture Coupling Between Two Concentric Coaxial Lines	5
	B. Aperture Leakage to the Inner Coaxial Line	10
	C. Wall-Thickness Effect for Small Holes	14
	D. Wall Thickness Effect for Circumferential Slit	15
	E. Lumped-Circuit Model of Connector Leakage	18
	F. Waveguide Model of Connector Leakage	21
III	TRANSMISSION-LINE PROPAGATION OF LEAKAGES	23
	A. Uniform Transmission Line with Sources	23
	B. Arbitrarily Terminated Uniform Transmission Line	27
	C. Transmission Line with Series-Voltage Source-- Voltage-Source Green's Function	31
	D. Transmission Line with Shunt-Current Source-- Current-Source Green's Function	33
	E. Transmission Lines Terminated in Characteristic Impedance	36
	F. Coaxial-Cable Leakage	37

G. Special Application	41
H. Example of Leakage from Two Apertures	44
IV CONCLUSIONS	53
REFERENCES	55

ILLUSTRATIONS

Figure 1	Aperture in Double Concentric Coaxial Line	5
Figure 2	Designation of Voltages and Currents	7
Figure 3	Equivalent Source Representation of Aperture	13
Figure 4	Circumferential Slit	15
Figure 5	Connector Model	19
Figure 6	Waveguide Model of Connector	21
Figure 7	Decomposition of Transmission Line	28
Figure 8	Point Series-Voltage Source	31
Figure 9	Point Shunt-Current Source	32
Figure 10	Coaxial Cable with Two Apertures	44
Figure 11	Relative Coupling of Two Holes in a Coaxial Line with an Infinitely Thin Conductor	51
Figure 12	Coupling Through Circular Holes in an Infinitely Thin Outer Conductor of an Air Coaxial Line	52

TABLES

Table 1	Values of the Polarizabilities of Small Holes	3
---------	---	---

I INTRODUCTION

Analysis of RF leakage into a shielded cable system is circumscribed by the unsatisfactory description of apertures in seams, joints, and connectors through which leakage predominantly occurs. Nevertheless, it is convenient to describe the leakage process in terms of aperture constants called the electric and magnetic polarizabilities. Measured leakage data can then be approximated by a synthesis of leakage expressions with empirically deduced aperture constants. Leakage measurements are usually obtained at the ends of the cable system that may be removed from the aperture. Hence, another aspect of the cable-system leakage analysis is to determine the propagation of leakage effects within the cable system.

A shielded cable system consists of many conductors within an electromagnetic shield. Furthermore, in a cable system having a trunk with several branches, the number of conductors in the branches is not the same as the number in the trunk, and many conductors go from one end of a branch through the trunk to the end of another branch, using only a portion of the cable system. Although such a cable system is to be evaluated for leakage, the more complicated analysis of the effects of leakage to each conductor and of propagation through the cable system, using multiconductor-transmission-line analysis, does not appear to be justified at this time. For the purpose of developing measurement and evaluation methods it is sufficient to investigate one cable segment, where many separately insulated conductors are treated as a single inner conductor and the shield is treated as the outer conductor of a coaxial line.

Electrical leakage through a small aperture is presented in terms of electric-dipole moments^{1*} excited by electric fields perpendicular to the plane of the aperture, and magnetic-dipole moments excited by magnetic fields tangential to the plane of the aperture. The electric dipole moment is proportional to the electric polarizability, P , which depends on the dimensions of the aperture. The magnetic-dipole moment is proportional to the magnetic polarization, M , for a circular aperture, but in other apertures the magnetic-dipole moment is also a function of the shape of the aperture. Convenient orthogonal coordinates for the aperture are chosen and the magnetic polarizabilities are determined along these coordinates. The magnetic field is resolved into components along these coordinates, and the magnetic-dipole moments are proportional to components of the magnetic field and the magnetic polarizability along the coordinate directions. Table 1 lists the polarizabilities of a simple aperture in a plane wall of zero thickness. Generally, apertures will not assume these simple forms, and empirical expressions to characterize the apertures will be necessary to fit the measured results. The expressions in the table serve as a guide to the allocation of empirical polarizabilities.

The present analysis of leakage into a shielded cable begins with the shielded cable as the inner coaxial line of a double concentric coaxial line with aperture leakage occurring across the common conductor of the inner and the outer coaxial lines. The configuration was chosen because an equivalent-circuit representation for it is available² and is readily extendable to the analysis of a coaxial line with current flowing on the exterior surface of the outer shield. The aperture leakage is

* References are listed at the end of the report.

Table 1

VALUES OF THE POLARIZABILITIES OF SMALL HOLES*

	M_1	M_2	P
Circle of radius r	$\frac{4}{3} r^3$	$\frac{4}{3} r^3$	$\frac{2}{3} r^3$
Ellipse [†] of eccentricity $\epsilon = \sqrt{1 - \left(\frac{b}{a}\right)^2}$	$\frac{\pi}{3} \frac{ab^2 \epsilon^2}{(1 - \epsilon^2)(F - E)}$	$\frac{\pi}{3} \frac{ab^2 \epsilon^2}{E - (1 - \epsilon^2)F}$	$\frac{\pi}{3} \frac{ab^2}{E}$
Long narrow ellipse ($a \gg b$)	$\frac{\pi}{3} \frac{a^3}{\ln\left(\frac{4a}{b}\right) - 1}$	$\frac{\pi}{3} ab^2$	$\frac{\pi}{3} ab^2$
Slit [‡] of width d and length L		$\frac{\pi}{16} Ld^2$	$\frac{\pi}{16} Ld^2$

* Marcuvitz (Ref. 2, p. 378), gives the polarizabilities for a circumferential slit of width d and circumference $2\pi R_2$, when R_2 is the radius, as

$$P = \frac{\pi d^2}{16}, \quad M_1 = -\frac{\lambda^2}{8\pi \ln \frac{4\lambda}{\pi d \gamma}}, \quad \gamma = 1.781, \quad \lambda = \text{wavelength}.$$

[†] F and E are the complete elliptic integrals of the first and second kind, respectively:

$$F(\epsilon) = \int_0^{\pi/2} \frac{d\varphi}{\sqrt{1 - \epsilon^2 \sin^2 \varphi}},$$

$$E(\epsilon) = \int_0^{\pi/2} d\varphi \sqrt{1 - \epsilon^2 \sin^2 \varphi}.$$

The polarizability M_1 is for the magnetic field parallel to the major semiaxis a; M_2 is for the field parallel to the minor semiaxis b.

[‡] The magnetic field is transverse to the slit and constant along the length.

Source: Ref. 1.

represented by a zero-impedance voltage source in series and a zero-admittance current source in shunt at the aperture location in the coaxial line.

An analysis is presented, determining voltages and currents propagated along the coaxial line from the aperture. For arbitrarily terminated coaxial lines, the results would be cumbersome without the use of voltage-source and current-source Green's functions to obtain a compact and more interpretable expression. The Green's functions are solutions of the transmission line with point sources located at the apertures.

The results could be written into a computer program to determine the effect of aperture leakages across the terminals of a coaxial line, excited by a current in the exterior shield. Because of the bundling of many conductors into a single conductor such a computer program was not written, but the analysis suggested measurement methods to evaluate leakage effects in a cable system.

II APERTURE LEAKAGE AND EQUIVALENT SOURCES

A. Aperture Coupling Between Two Concentric Coaxial Lines

The equivalent circuit of the aperture coupling between two concentric coaxial line forms the basis for investigating leakage from external fields and currents into the coaxial line. The equivalent circuit and the values of the circuit parameters for infinitely thin coupling walls are given by Marcuvitz² for TEM modes, and are illustrated in Figure 1.

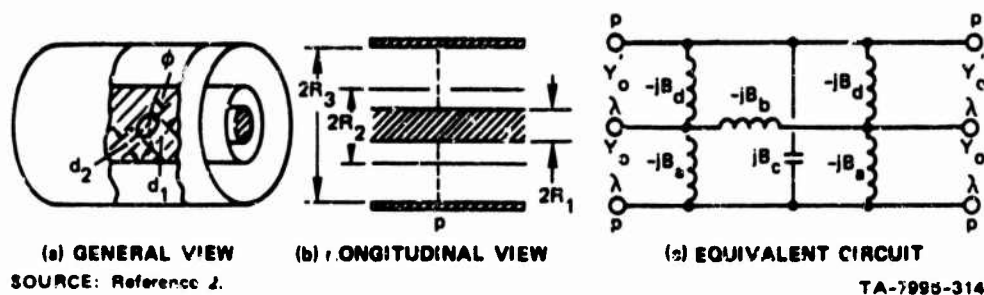


FIGURE 1 APERTURE IN DOUBLE CONCENTRIC COAXIAL LINE.

Equivalent-circuit parameters at the common central reference plane, p , in Figure 1 are given by

$$\frac{Y'_0}{Y_0} = \frac{\ln \frac{R_2}{R_1}}{\ln \frac{R_3}{R_2}}, \quad (1)$$

$$\frac{B_a}{Y_0} = \frac{P}{2\lambda R_2^2 \ln \frac{R_2}{R_1}} \left(1 + \frac{\ln \frac{R_2}{R_1}}{\ln \frac{R_3}{R_2}} \right) = \frac{\omega P(Y_0 + Y'_0)}{4\pi c R_2^2 \ln \frac{R_2}{R_1}} \quad (2)$$

$$\frac{B_b}{Y_0} = \frac{2\lambda R_2^2 \ln \frac{R_2}{R_1}}{M} = \frac{2\pi c R_2^2 \ln \frac{R_2}{R_1}}{\omega M} \quad (3)$$

$$\frac{B_c}{Y_0} = \frac{B_a}{Y_0} \frac{2}{\ln \frac{R_3}{R_2} + 1 + \frac{\ln \frac{R_2}{R_1}}{\ln \frac{R_3}{R_2}}} \quad (4)$$

$$\frac{B_d}{Y_0} = \frac{B_a}{Y_0} \frac{\ln \frac{R_2}{R_1}}{\ln \frac{R_3}{R_2}} \quad (5)$$

where

c = Propagation velocity

P = Electric polarizability

M = Magnetic polarizability

λ = Wavelength

Y_0 = Characteristic admittance of inner coaxial line

Y'_0 = Characteristic admittance of outer coaxial line.

The circuit is sufficiently complicated so that it is difficult both to describe and to apply. However, if the circuit is considered in terms of zero-impedance voltage and zero-admittance current generators, applicability becomes a little more apparent. Although the equivalent circuit is for coupling through an infinitely thin aperture, a radius R'_2 is introduced for the inner radius of the outer coaxial line, in order to consider the effect of finite thickness later on. Since $R_2 \approx R'_2$, we could use either R_2 or R'_2 in the values for the equivalent-circuit parameters, where the choice of R_2 or R'_2 depends on its appropriateness in the expression. The equivalent circuit with current and voltage designation is illustrated in Figure 2.

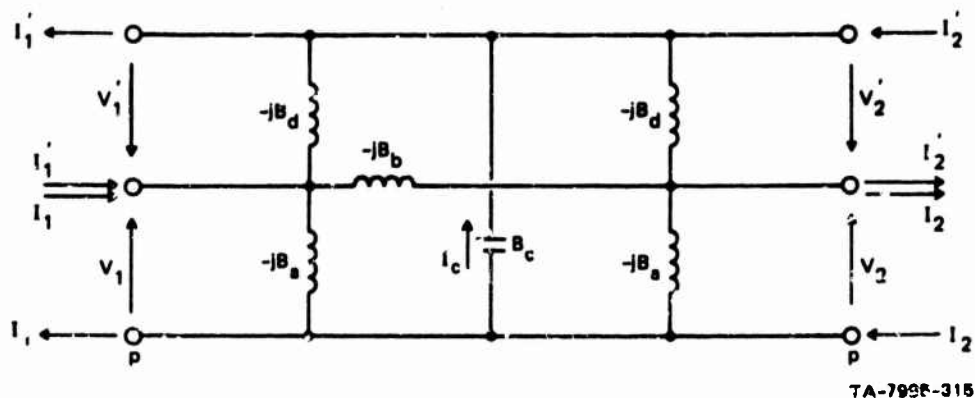


FIGURE 2 DESIGNATION OF VOLTAGES AND CURRENTS

Equivalent zero-impedance voltage and zero-admittance current generators enable the leakages coupled into transmission lines to be represented by uncoupled transmission lines with generator sources simulating the coupled quantities. The following current and voltage expressions are obtained for reference in later sections. The current through $Y_a = -jB_a$ connected across voltage, V_1 , is, from Eq. (2):

$$I_{a1} = -jB_a V_1 = I_{a10} + I_{a10}' \quad (6)$$

where

$$I_{a10} = \frac{j\omega P Y_0}{4\pi c R_2^2 \ln \frac{R_2}{R_1}} V_1 \quad (7)$$

$$I_{a10}' = - \frac{j\omega P Y_0'}{4\pi c R_2^2 \ln \frac{R_2}{R_1}} V_1 \quad (8)$$

Similarly, from Eq. (3), with voltage V_1' across $Y_d = -jB_d$,

$$I_{d1}' = -jB_d V_1' = - \frac{j\omega P Y_0}{4\pi v R_2^2 \ln \frac{R_2}{R_1}} V_1' - \frac{j\omega P Y_0'}{4\pi c R_2^2 \ln \frac{R_3}{R_2}} V_1' = I_{a10}' + I_{a10}' \quad (9)$$

from Eq. (2) with voltage V_2 across $Y_a = -jB_a$,

$$I_{a2} = -jB_a V_2 = - \frac{j\omega P Y_0}{4\pi c R_2^2 \ln \frac{R_2}{R_1}} V_2 - \frac{j\omega P Y_0'}{4\pi c R_2^2 \ln \frac{R_2}{R_1}} V_2 = I_{a20} + I_{a20}' \quad (10)$$

and from Eq. (5) with voltage V_2' across $Y_d = -jB_d$,

$$\begin{aligned} I_{d2}' &= -jB_d V_2' = - \frac{j\omega P Y_0}{4\pi c R_2^2 \ln \frac{R_3}{R_2}} V_2' - \frac{j\omega P Y_0'}{4\pi v T_2' \ln \frac{R_3}{R_2}} V_2' \\ &= I_{d20}' + I_{d20}' \end{aligned} \quad (11)$$

The current, I_b , flowing through $Y_b = -jB_b$ is

$$I_b = I_i - I_{a1} + (I'_1 - I'_{d1}) = I_{b1} + I'_{b1} \quad (12)$$

The equivalent zero-impedance voltage generator, V_b , obtained as the voltage across $Y_b = -B_b$, when current I_b is flowing through it, is

$$\begin{aligned} V_b = \frac{I_b}{-jB_b} &= \frac{j\omega M}{2\pi c Y_0 R_2^2 \ln \frac{R_2}{R_1}} I_b \\ &= \frac{j\omega M Z_0}{2\pi c R_2^2 \ln \frac{R_2}{R_1}} I_{b1} + \frac{j\omega M Z_0}{2\pi c R_2^2 \ln \frac{R_2}{R_1}} I'_{b1} \end{aligned} \quad (13)$$

The equivalent zero-admittance current generator, I_c , associated with $Y_c = jB_c$ is the current flowing through $Y_c = B_c$, when the voltage $-V_1 + V'_1$ is impressed across it, and is given as

$$\begin{aligned} I_c = jB_c (-V_1 + V'_1) &= \frac{j\omega P}{2\pi c} \left[\frac{Y'_0}{R_2^2 \ln \frac{R_2}{R_1}} (-V_1) + \frac{Y_0}{R_2'^2 \ln \frac{R_2}{R_1}} V'_1 \right] \\ &= I_{c1} + I'_{c1} \end{aligned} \quad (14)$$

The voltages and currents at the aperture are related by

$$I = Y_p V \quad (15)$$

where Y_p is the admittance of the line at $z = p$. Thus, the magnetic and electric fields at the aperture are related to voltages and currents at the aperture by

$$I = 2\pi R_2 H_\varphi(R_2) = \frac{2\pi R_2}{\zeta} E_R(R_2) = Y_p V \quad (16)$$

$$I' = 2\pi R_2' H_\varphi(R_2') = \frac{2\pi R_2'}{\zeta} E_R(R_2') = Y_p' V' \quad (17)$$

where

$$\zeta = \sqrt{\mu/\epsilon}.$$

B. Aperture Leakage to the Inner Coaxial Line

Leakage to the inner coaxial line is determined by considering only the outer voltage V_1' , and current I_1' , at the aperture. When the aperture is small, the voltages and currents coupled into the inner line will be a very small fraction of the driving voltage or current, and therefore its contribution being secondary by comparison may be neglected. Then from the Eq. (13), zero-impedance voltage source, V_b , becomes

$$V_b = V_{b1} = \frac{j\omega M}{2\pi c Y_0 R_2^2 \ln \frac{R_2}{R_1}} (I_1' - I_{d1}') \quad (18)$$

and from Eq. (14), since $V_1' \gg V_1$, the zero-admittance current source, I_c , becomes

$$I_c = I'_{c1} = \frac{j\omega^2 Y_0}{2\pi c R_2'^2 \ln \frac{R_3}{R_2}} V'_1 \quad (19)$$

But from Eq. (9),

$$\begin{aligned} I'_{d1} &= - \frac{j\omega P}{4\pi c R_2'^2 \ln \frac{R_3}{R_2}} (Y_0 + Y'_0) V'_1 \\ &= - \frac{j\omega P}{4\pi c R_2'^2 \ln \frac{R_3}{R_2}} \left(\frac{Y_0 + Y'_0}{Y'_p} \right) I'_1 \quad (20) \end{aligned}$$

A circularly uniform current flowing on the outer shield of a single coaxial cable is obtained by letting R_3 , the radius of the outer cylindrical tube, approach infinity in Eq. (20). This decreases I'_{d1} so that eventually

$$|I'_{d1}| \ll |I'_1| \quad (21)$$

and consequently I'_{d1} may be neglected. Since

$$Y_0 = \frac{2\pi}{\epsilon \ln \frac{R_2}{R_1}} = \frac{2\pi}{\mu c \ln \frac{R_2}{R_1}} \quad (22)$$

the zero-impedance voltage source given by Eq. (18), is simplified to

$$V_b = \frac{j\omega \mu M}{4\pi R_2^2} I_1' \quad (23)$$

The zero-admittance current source, I_c of Eq. (19), with the relation $I_1' = Y_p' V_1'$, becomes

$$I_c = \frac{j\omega P}{2\pi c R_2^2 \ln \frac{R_3}{R_2}} \frac{Y_0}{Y_p'} I_1' \quad (24)$$

and, with Eq. (1), becomes

$$I_c = \frac{j\omega P}{2\pi c R_2^2 \ln \frac{R_2}{R_1}} \frac{Y_0'}{Y_p'} I_1'$$

If $Y_p' = Y_0'$, then I_1' is the current flowing in the positive z direction without reflection, so that

$$\begin{aligned} I_c &= \frac{j\omega P}{2\pi c R_2^2 \ln \frac{R_2}{R_1}} I_1' \\ &= \frac{j\omega \mu P Y_0}{4\pi R_2^2} I_1' \end{aligned} \quad (25)$$

If there is reflection, I_c would have a value less than twice the value given by the equation. Since R_3 is not present in these expressions,

the expression is applicable to the case of I'_1 flowing on the exterior surface of a coaxial line.

The equivalent generator representation obtained through a series of approximations for small-aperture coupling gives the result depicted in Figure 3.

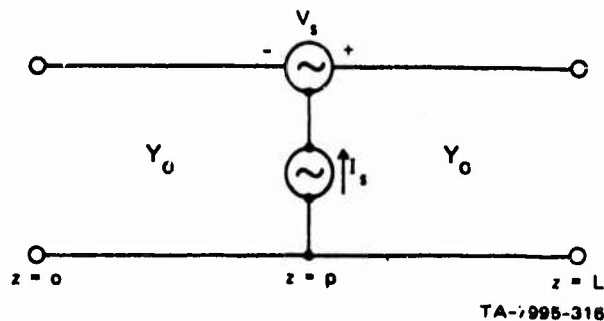


FIGURE 3 EQUIVALENT SOURCE REPRESENTATION OF APERTURE

The terminals represent the ends of the inner coaxial line and the generators represent the coupled zero-impedance voltage and zero-admittance current sources where the transfer impedance Z_p is defined by

$$V_s = V_b = Z_p I'_1 = \frac{j\omega \mu M}{4\pi R_2^{2/2}} I'_1 \quad (26)$$

and the transfer function T_p is defined by

$$I_s = I_c = T_p I'_1 = \frac{j\omega \mu P Y_0}{4\pi R_2^{2/2}} I'_1 \quad (27)$$

Z_p and T_p are for coupling holes in infinitely thin walls, but in practical applications finite wall thickness must be considered, as discussed in the next section.

C. Wall-Thickness Effect for Small Holes

Finite wall thickness reduces the coupling effect and hence decreases the value of the transfer impedance and function. The electric polarizability, P , in the equivalent current generator, I_s , determines the magnitude of the lowest longitudinal E field mode in the aperture, and the magnetic polarizability, M , determines the magnitude of the lowest longitudinal H field mode in the aperture. The lowest E and H modes have wavelengths longer than the cutoff wavelength, so the fields are attenuated in the aperture. For wall thickness $T = R'_2 - R_2$, the attenuation factor is given by $e^{-\gamma T}$ where γ is the complex-mode propagation constant given by

$$\begin{aligned}\gamma &= \sqrt{k_c^2 - k^2} = \sqrt{\left(\frac{2\pi}{\lambda_c}\right)^2 - \left(\frac{2\pi}{\lambda}\right)^2} \\ &= \sqrt{\left(\frac{2\pi}{\lambda_c}\right)^2 + \left(\frac{j\omega}{c}\right)^2} = \alpha + j\beta\end{aligned}\quad (28)$$

where λ_c is the cutoff wavelength of the mode. Including the wall-thickness factor, the expressions for transfer impedance and transfer function become

$$Z_p = \frac{j\omega \mu M e^{-\gamma_H T}}{4\pi R'^2} \quad (29)$$

and

$$T_p = \frac{j\omega\mu P Y_0 e^{-\gamma_E T}}{4\pi^2 R'^2} \quad (30)$$

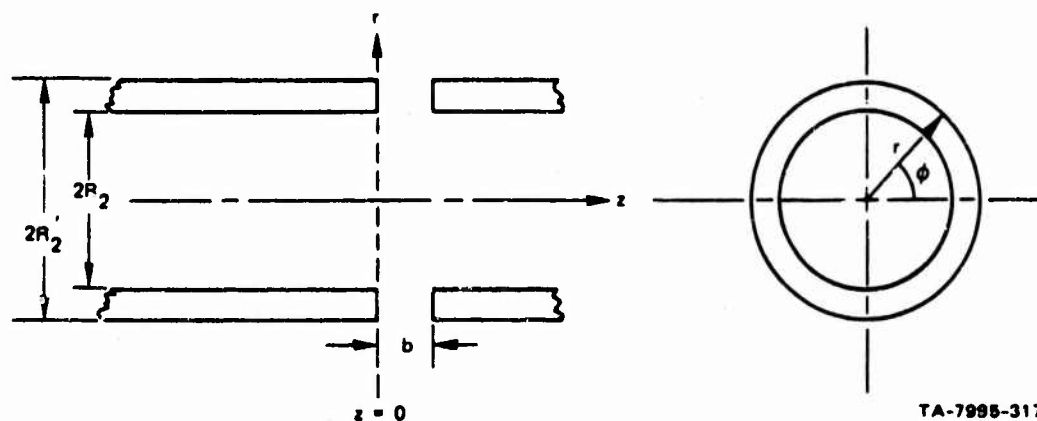
where

γ_H = Complex propagation factor for the lowest H mode

γ_E = Complex propagation factor for the lowest E mode.

D. Wall Thickness Effect for Circumferential Slit

The effect of thickness, $T = R'_2 - R_2$, for the circumferential slit in the concentric conductor between the inner and outer coaxial cable is obtained by considering the slit as a radial waveguide as shown in Figure 4.



TA-7995-317

FIGURE 4 CIRCUMFERENTIAL SLIT

Since the slit is excited by a radial electric field and a circular magnetic field, an E_{01} mode and not the lowest E_{00} mode is excited in the slit. The electric and magnetic fields in the slit are given by Marcuvitz (Ref. 2, p. 90) as

$$\left. \begin{aligned}
 E_z &= -\frac{2V'_1}{b} \cos \frac{\pi}{b} z, & H_z &= 0 \\
 E_\phi &= 0, & H_\phi &= \frac{I'_1}{2\pi r} \cos \frac{\pi}{b} z \\
 E_r &= -j \frac{\zeta I'_1}{2rkb} \sin \frac{\pi}{b} z
 \end{aligned} \right\} \quad (31)$$

where the mode voltages and currents satisfy the transmission-line equations

$$\left. \begin{aligned}
 \frac{dV'_1}{dr} &= -jk_1 Z'_1 I'_1 \\
 \frac{dI'_1}{dr} &= -jk_1 Y'_1 V'_1
 \end{aligned} \right\} \quad (32)$$

where

$$\left. \begin{aligned}
 Z'_1 &= \frac{1}{Y'_1} = \frac{\zeta b}{4\pi r} \frac{k_1}{k} \\
 k_1 &= \sqrt{k^2 - \left(\frac{\pi}{b}\right)^2} = j \sqrt{\left(\frac{j\omega}{c}\right)^2 + \left(\frac{2\pi}{\lambda_c}\right)^2} \\
 \lambda_c &= 2b
 \end{aligned} \right\} \quad (33)$$

The second-order differential equations for V'_1 and I'_1 become

$$\frac{1}{r} \frac{d}{dr} r \frac{dV'_1}{dr} + K_1^2 V'_1 = 0 \quad (34)$$

$$r \frac{d}{dr} \frac{1}{r} \frac{dI'_1}{dr} + k_1^2 V'_1 = 0$$

The usual method of expressing solutions to the above equations is to solve for V'_1 in terms of modified Bessel's or Hankel's function and use the first-order transmission-line equation to obtain a solution for I'_1 . The solution for I'_1 is needed to determine propagation behavior for E_r and H_ϕ .

An approximate and simpler treatment for cylinders with thin walls is possible since the r -variation in the second-order differential equation is small so that r may be set equal to the outer radius, R'_2 , of the cylinder, but I'_1 and V'_1 are still functions of r . Then the second-order differential equations become

$$\frac{d^2}{dr^2} I'_1 + k_1^2 I'_1 = 0 \quad (35)$$

with solutions of the form $e^{jk_1 r}$ and $e^{-jk_1 r}$ for waves propagating in the direction of decreasing and increasing r , respectively. Since we are interested in leakage into the tubular conductor or in the direction of decreasing r , the amplitude-variation factor to allow for the thickness, $T = R'_2 - R_2$, is

$$e^{-jk_1 T} = e^{-\sqrt{\left(\frac{j\omega}{c}\right)^2 + \left(\frac{2\pi}{\lambda_c}\right)^2} T} \quad (36)$$

E. Lumped-Circuit Model of Connector Leakage

The lumped-circuit model of connector leakage assumes that the electrical lengths associated with the connectors are small, so that lumped-circuit considerations are adequate in the determination of the current exciting the aperture. A circumferential slit in the connector is considered to be the aperture. If metal-to-metal contact exists in the circumferential slit, then the space between contacts could be modeled as a circular, elliptical, or rectangular aperture. The aperture case is treated in the next section. The purpose of these treatments is to suggest models that may be used to represent experimental results. In all cases, the model oversimplifies the actual field configuration in the space between threads and bushing of the connector.

A longitudinal cross section of a connector model is illustrated in Figure 5. At the connector, the model shows that the outer conductor of the coaxial lines has a circumferential slit with gap width, b , at $z = p$. The schematic illustrates the admittances y_{12} , y_{13} , and y_{23} , existing between components of a connector, where 1 refers to the outer coaxial cable connector on the left, 2 refers to the outer coaxial cable connector on the right; and 3 refers to the connector bushing that reduces the gap, b , between the left and right coaxial line. Admittances Y_{12} , Y_{13} , and Y_{23} or their reciprocal, impedances Z_{12} , Z_{13} , and Z_{23} , are values measured between the respective components of the connector by connecting

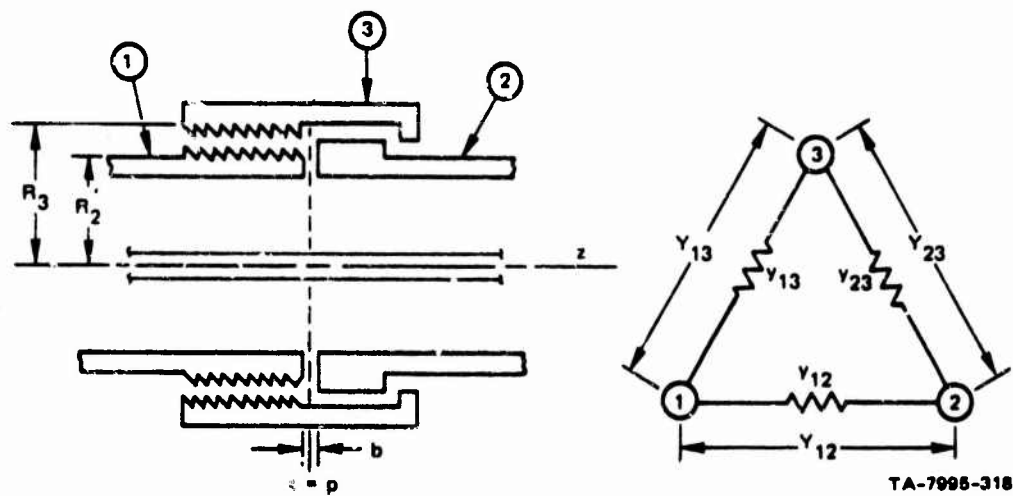


FIGURE 5 CONNECTOR MODEL

an admittance or impedance meter. The relationships between measured admittances and admittances between components of a connector are:

$$Y_{12} = \frac{K}{y_{13} + y_{23}}, \quad (37)$$

$$Y_{13} = \frac{K}{y_{12} + y_{23}}, \quad (38)$$

$$Y_{23} = \frac{K}{y_{12} + y_{13}}, \quad (39)$$

where

$$K = y_{12}y_{13} + y_{12}y_{23} + y_{13}y_{23}. \quad (40)$$

Solving for y_{12} , y_{13} , and y_{23} in terms of the measured values gives

$$y_{12} = \frac{K}{2} (Z_{13} + Z_{23} - Z_{12}) \quad (41)$$

$$y_{13} = \frac{K}{2} (Z_{12} + Z_{23} - Z_{13}) \quad (42)$$

$$y_{23} = \frac{K}{2} (Z_{12} + Z_{13} - Z_{23}) \quad (43)$$

If a current I flows on the outer surface of the coaxial line, a portion I_{12} of the current flows across admittance y_{12} , and thereby couples through the circumferential slit of gap, b , into the coaxial line. Now,

$$I = I_{12} + I_{13} \text{ and } I_{13} = I_{32} \quad (44)$$

and since the voltage across y_{12} is equal to the voltage across y_{13} and y_{23} , we have that

$$\frac{I_{12}}{y_{12}} = \frac{(I - I_{12})(y_{13} + y_{23})}{y_{13}y_{23}} \quad (45)$$

The fraction of the current I flowing through y_{12} in terms of measured impedances is

$$\frac{I_{12}}{I} = \frac{2Z_{12}(Z_{13} + Z_{32} - Z_{12})}{(Z_{12} + Z_{13} + Z_{23})^2 - 2(Z_{12}^2 + Z_{13}^2 + Z_{23}^2)} \quad (46)$$

Results of measurements on connectors indicate that Z_{12} , Z_{13} , and Z_{23} have essentially zero resistance for frequencies to 100 MHz. Hence, the conclusion is that metallic contact exists between Parts 1 and 2 and between Parts 2 and 3 (see Figure 5), so that leakage through these connectors must be due to aperture coupling.

F. Waveguide Model of Connector Leakage

The waveguide model of connector leakage utilizes the principle of aperture leakage through thick walls. Figure 6 illustrates waveguides formed in the connector because of metallic contact between the connector bushing and the connector, which functions as an extension of the coaxial line. Three arc-shaped waveguides are illustrated with a cross section of mean width w_1 , w_2 , and w_3 , and height $h = R_3 - R_2'$, and with length l_p .

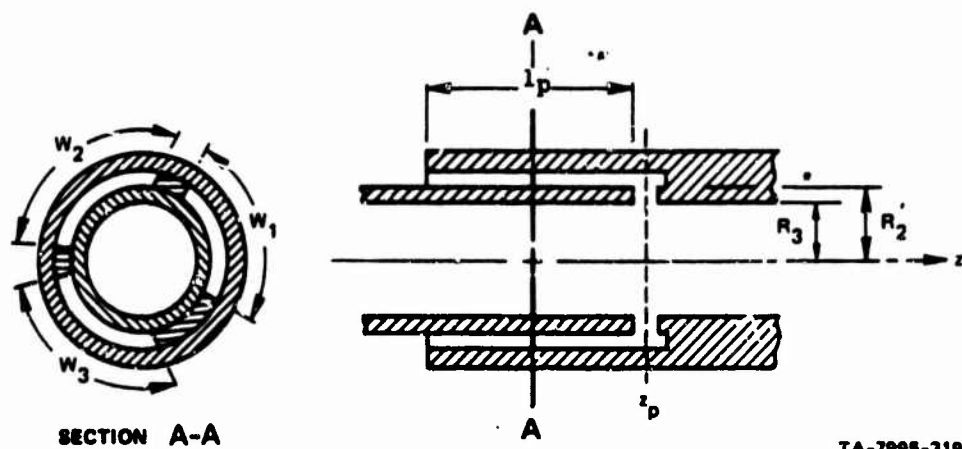


FIGURE 6 WAVEGUIDE MODEL OF CONNECTOR

The length, l_p , is short enough so that the current flowing on the outer aperture surface of the waveguide may be assumed to be the current at z_p . However, the length, l_p , is retained to compute the attenuation through the waveguide and becomes the aperture wall thickness to account for the wall-thickness factor.

The dipole moments, excited in the connector waveguide model, is slightly different from apertures in the coaxial surface since the apertures are in a plane surface perpendicular to the circular coaxial surface. The magnetic-dipole moment excited by current on the outer surface of the coaxial line is essentially due to the magnetic field in line with the long (major) axis of the aperture. The electric-dipole moment would be smaller since the electric field perpendicular to the aperture would be smaller than that normally existing on the surface of the coaxial line.

It is evident that many types of leakage behavior could be approximated with appropriate choices of waveguide cross sections and lengths. The discussion of leakage provides a semi-quantitative description of the connector leakage process, even though physical description of the apertures in a connector is not adequate to permit a more thorough analytical treatment.

III TRANSMISSION-LINE PROPAGATION OF LEAKAGES

This section discusses a method for treating transmission lines excited by aperture leakage that can be represented by zero-impedance series voltage and zero-admittance shunt-current sources. The resulting expressions would be unwieldy and uninformative unless voltage- and current-source Green's functions³ are used. Consequently, this method* is reviewed and parameters are defined to enable the final results to be usable.

A. Uniform Transmission Line with Sources

The uniform-transmission-line equations with a zero-impedance voltage source, V_s , in series along the line and a zero-admittance current source I_s shunted across the line are given by

$$\left. \begin{aligned} \frac{dV}{dz} &= -ZI + V_s \\ \frac{dI}{dz} &= -YV + I_s \end{aligned} \right\} \quad (47)$$

where Z and Y are the distributed series impedance and shunt admittance per unit length of line.

The second-order differential equation in V or I is obtained by differentiating the equations and making appropriate substitution. However, differentiation of the sources may be avoided by using the linearity

* Reference 3, pp. 102-111.

property of the equations and forming two sets of two equations as follows:

$$\left. \begin{aligned} \frac{dV^V}{dz} &= -ZI^V + V_s \\ \frac{dI^V}{dz} &= -YV^V \end{aligned} \right\} \quad (48)$$

$$\left. \begin{aligned} \frac{dV^I}{dz} &= -ZI^I \\ \frac{dI^I}{dz} &= -YV^I + I_s \end{aligned} \right\} \quad (49)$$

where the superscript V is associated with voltage and current from voltage source V_s , with the current source $I_s = 0$. Conversely, the superscript I is associated with voltage and current from current source I_s , with the voltage source $V_s = 0$. Summing the two sets of equations gives

$$\left. \begin{aligned} \frac{d(V^V + V^I)}{dz} &= -Z(I^V + I^I) + V_s \\ \frac{d(I^V + I^I)}{dz} &= -Y(V^V + V^I) + I_s \end{aligned} \right\} \quad (50)$$

which are the original equations, in which

$$\left. \begin{aligned} V &= V^V + V^I \\ I &= I^V + I^I \end{aligned} \right\} \quad (51)$$

The second-order differential equations obtained from Eqs. (48) and (49) are

$$\left. \begin{aligned} \frac{d^2 V}{dz^2} - \gamma^2 I V &= -\gamma V_s \\ \frac{d^2 I}{dz^2} - \gamma^2 V I &= -Z I_s \end{aligned} \right\} \quad (52)$$

where

$$\gamma = \sqrt{ZY} \quad (53)$$

The solutions of the differential equations driven by the zero-impedance voltage source V_s are obtained by first considering the case in which a zero-impedance unity point voltage source is located at $z = z'$, since this solution is generally easier to obtain. The desired solution is then obtained by superposition. The unit point voltage source is described by

$$V_s = \delta(z - z') \quad (54)$$

and the forcing function becomes $-\gamma\delta(z - z')$. If the forcing function were $\delta(z - z')$, the Green's function $\phi_G^I(z, z')$ would satisfy the second-order differential equation

$$\frac{d^2 \phi_G^I}{dz^2} - \gamma^2 \phi_G^I = \delta(z - z') \quad (55)$$

The forcing function, $-\gamma\delta(z - z')$, gives the voltage-source Green's function

$$I_G^V(z, z') = -\gamma\phi_G^I(z, z') \quad (56)$$

which satisfies the second-order differential equation.

The solution, I^V , to the driving function, γV_s , results from superposition of currents due to voltage sources at different locations along the line, and is

$$I^V(z) = \int V_s(z') I_G^V(z, z') dz' \quad (57)$$

The solution for voltage, V^V , is found from

$$V_G^V(z) = -\frac{1}{\gamma} \frac{dI_G^V(z, z')}{dz} \quad (58)$$

with the result that

$$V^V(z) = \int V_s(z') V_G^V(z, z') dz' \quad (59)$$

Similarly, the solutions to the zero-admittance current source, I_s , shunted across the line are

$$V^I(z) = \int I_s(z') V_G^I(z, z') dz' \quad (60)$$

$$I^I(z) = \int I_s(z') I_G^I(z, z') dz' \quad (61)$$

where the current-source Green's functions are

$$V_G^I(z, z') = -Z\phi_G^I(z, z') \quad (62)$$

and

$$I_G^I(z, z') = -\frac{1}{Z} \frac{dV_G^I(z, z')}{dz} \quad (63)$$

The solutions V^V , I^V , V^I , and I^I are in terms of voltage-source and current-source Green's functions, which are computed in the following sections.

B. Arbitrarily Terminated Uniform Transmission Line

This section reviews the transmission-line definitions and solutions to provide continuity with later sections where point driving sources are introduced to satisfy boundary conditions. The uniform transmission line of characteristic impedance Z_0 and length L is terminated in impedances $Z_1 = 1/Y_1$ at $z = 0$ and $Z_2 = 1/Y_2$ at $z = L$. A zero-impedance series-voltage or zero-admittance shunt-current source discontinuity will be introduced at $z = z'$ in later sections. Consequently, the line is divided into the two source-free lines illustrated in Figure 7, where the line from $z = 0$ to $z = z'$ is called Region 1 and the line from $z = z'$ to $z = L$ is called Region 2. The voltage, V_1 , and current, I_1 , in Region 1 will be expressed in terms of variables and parameters occurring in Region 1. Similarly, the voltage V_2 , and current, I_2 , in Region 2 will be expressed in terms of variables and parameters occurring in Region 2.

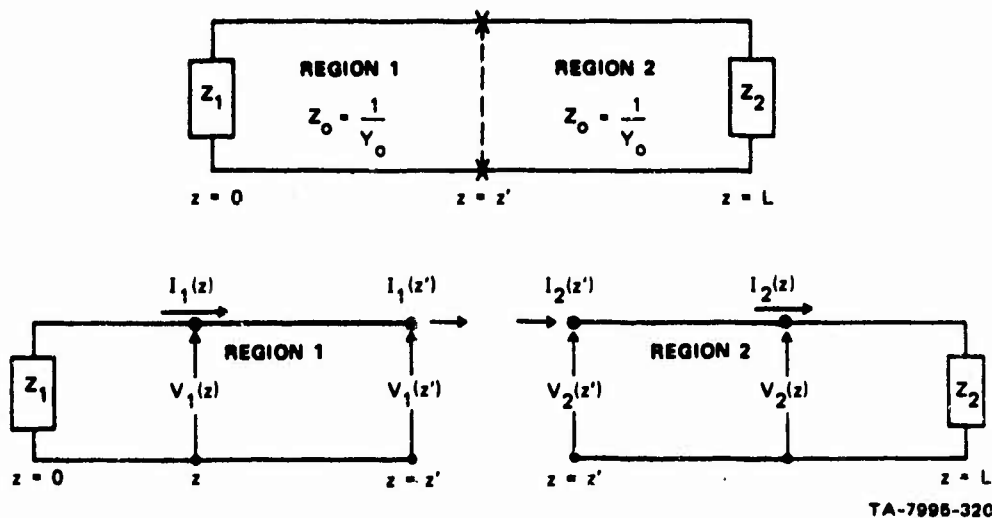


FIGURE 7 DECOMPOSITION OF TRANSMISSION LINE

In Region 1, the voltage and current may be expressed in terms of the forward (positive z direction) and reverse (negative z direction) propagating voltages, V_{1f} and V_{1r} , and currents, I_{1f} and I_{1r} , evaluated at $z = 0$ to give

$$V_1(z) = V_{1r}e^{\gamma z} + V_{1f}e^{-\gamma z} \quad (64)$$

$$I_1(z) = I_{1r}e^{\gamma z} + I_{1f}e^{-\gamma z} \quad (65)$$

From

$$V_1 = -\frac{1}{Y} \frac{dI_1}{dz} = -\frac{\gamma}{Y} (I_{1r}e^{\gamma z} - I_{1f}e^{-\gamma z}) \quad (67)$$

and equating coefficients of the exponential terms in the expression for V_1 , we have

$$V_{1r} = -\frac{\gamma}{Y} I_{1r} = -\frac{I_{1r}}{Y_0} \quad (68)$$

and, similarly,

$$V_{1f} = \frac{I_{1f}}{Y_0} \quad (69)$$

Consequently, the current equation may be written as

$$I_1(z) = Y_0(-V_{1r}e^{\gamma z} + V_{1f}e^{-\gamma z}) \quad (70)$$

At $z = 0$, the voltage developed across Z_1 by $I_1(0)$ is in opposite polarity to the voltage convention along the line. Hence,

$$Z_1 = -\frac{V_1(0)}{I_1(0)} = -\frac{V_{1r} + V_{1f}}{Y_0(-V_{1r} + V_{1f})} = Z_0 \frac{1 + \rho_1}{1 - \rho_1} \quad (71)$$

where the voltage reflection coefficient is $\rho_1 = V_{1f}/V_{1r}$, since V_{1r} at $z = 0$ is the incident voltage from a source at $z = z'$. ρ_1 becomes expressed in terms of impedances and admittances in the usual way as

$$\rho_1 = \frac{Z_1 - Z_0}{Z_1 + Z_0} = \frac{Y_0 - Y_1}{Y_0 + Y_1} \quad (72)$$

The voltage and current in Region 1 is now written as

$$V_1(z) = V_{1r}e^{\gamma z}(1 + \rho_1e^{-2\gamma z}) \quad (73)$$

$$I_1(z) = -Y_0V_{1r}e^{\gamma z}(1 - \rho_1e^{-2\gamma z}) \quad (74)$$

where V_{1r} is still an undetermined parameter.

Similarly, in Region 2, the voltages and currents are given by

$$V_2(z) = V_{2r} e^{\gamma z} + V_{2f} e^{-\gamma z} \quad (75)$$

$$\begin{aligned} I_2(z) &= I_{2r} e^{\gamma z} + I_{2f} e^{-\gamma z} \\ &= Y_0 \left(-V_{2r} e^{\gamma z} + V_{2f} e^{-\gamma z} \right) \end{aligned} \quad (76)$$

where V_{2f} , V_{2r} , I_{2f} , and I_{2r} are forward and reverse propagating voltages and currents evaluated at $z = 0$ if Region 2 extends back to $z = 0$, without intermediate sources. At $z = L$, the impedance Z_2 becomes related to the voltage-reflection coefficient, ρ_2 , which is given by the ratio of the reflected voltage, $V_{2r} e^{\gamma L}$, to the incident voltage, $V_{2f} e^{-\gamma L}$, since

$$Z_2 = \frac{V_2(L)}{I_2(L)} = \frac{V_{2f} e^{-\gamma L} \left(\frac{V_{2r}}{V_{2f}} e^{2\gamma L} + 1 \right)}{Y_0 V_{2f} e^{-\gamma L} \left(-\frac{V_{2r}}{V_{2f}} e^{2\gamma L} + 1 \right)} = Z_0 \frac{\rho_2 + 1}{-\rho_2 + 1} \quad (77)$$

Solving for ρ_2 gives

$$\rho_2 = \frac{Z_2 - Z_0}{Z_2 + Z_0} = \frac{Y_0 - Y_2}{Y_0 + Y_2} = \frac{V_{2r}}{V_{2f}} e^{2\gamma L} \quad (78)$$

Then, in terms of the undetermined parameter, V_{2f} , the voltages and currents in Region 2 may be written as

$$V_2(z) = V_{2f} e^{-\gamma z} \left[1 + \rho_2 e^{2\gamma(z-L)} \right] \quad (79)$$

$$I_2(z) = Y_0 V_{2f} e^{-\gamma z} \left[1 - \rho_2 e^{2\gamma(z-L)} \right] \quad (80)$$

The undetermined parameters V_{1r} and V_{2f} are determined in terms of voltage or current source introduced at $z = z'$, and thereby solutions are obtained for voltages and currents in Regions 1 and 2 in terms of voltage- and current-source Green's functions.

C. Transmission Line with Series-Voltage Source--Voltage-Source Green's Function

A zero-impedance point voltage source $V_s(z')$ in series with the line at $z = z'$ is depicted in Figure 8. The boundary conditions at $z = z'$ and their relationships to transmission-line parameters in

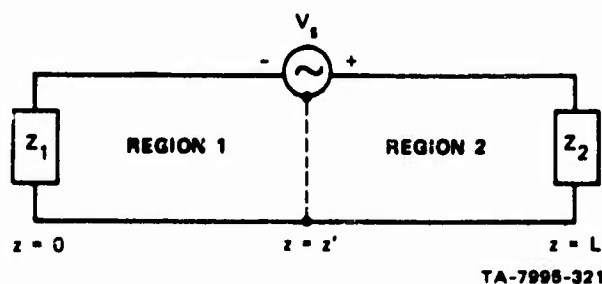


FIGURE 8 POINT SERIES-VOLTAGE SOURCE

Regions 1 and 2 [Eqs. (73), (74), (79), and (80)] are given by

$$\begin{aligned}
 V_2^V(z') - V_1^V(z') &= V_s^V(z') \\
 &= V_{2f}^V e^{-\gamma z'} \left[1 + \rho_2 e^{2\gamma(z'-L)} \right] - V_{1r}^V e^{\gamma z'} \left(1 + \rho_1 e^{-2\gamma z'} \right) \\
 I_2^V(z') - I_1^V(z') &= 0 \\
 &= Y_0 V_{2f}^V e^{-\gamma z'} \left[1 - \rho_2 e^{2\gamma(z'-L)} \right] + Y_0 V_{1r}^V e^{\gamma z'} \left(1 - \rho_1 e^{-2\gamma z'} \right)
 \end{aligned} \tag{81}$$

Solving for V_{1r}^V and V_{2f}^V gives

$$V_{1r}^V = - \frac{e^{-\gamma z'} \left[1 - \rho_2 e^{2\gamma(z'-L)} \right]}{\left(2 - \rho_1 \rho_2 e^{-2\gamma L} \right)} V_s^V(z') \tag{82}$$

$$V_{2f}^V = \frac{e^{\gamma z'} \left(1 - \rho_1 e^{-2\gamma x'} \right)}{2 \left(1 - \rho_1 \rho_2 e^{-2\gamma L} \right)} V_s^V(z') \tag{83}$$

The Green's-function solution for Regions 1 and 2 is obtained by setting $V_s(z') = 1$ and substituting the expression for V_{1r}^V and V_{2f}^V into Eqs. (73), (74), (79), and (80) for voltages and currents to give, in Region 1, where $z < z'$,

$$V_{1G}^V(z, z') = - \frac{\left[1 - \rho_2 e^{2\gamma(z'-L)} \right]}{2 \left(1 - \rho_1 \rho_2 e^{-2\gamma L} \right)} \left[e^{\gamma(z-z')} + \rho_1 e^{-\gamma(z+z')} \right] \tag{84}$$

$$V_{1G}^V(z, z') = \frac{Y_0 \left[1 - \rho_2 e^{2Y(z'-L)} \right]}{2 \left(1 - \rho_1 \rho_2 e^{-2YL} \right)} \left[e^{Y(z-z')} - \rho_1 e^{-Y(z+z')} \right] \quad (85)$$

and in Region 2, where $z > z'$,

$$V_{2G}^V(z, z') = \frac{\left(1 - \rho_1 e^{-2Yz'} \right)}{2 \left(1 - \rho_1 \rho_2 e^{-2YL} \right)} \left[e^{-Y(z-z')} + \rho_2 e^{Y(z+z'-2L)} \right] \quad (86)$$

$$I_{2G}^V(z, z') = \frac{\left(1 - \rho_1 e^{-2Yz'} \right)}{2 \left(1 - \rho_1 \rho_2 e^{-2YL} \right)} \left[e^{-Y(z-z')} - \rho_2 e^{Y(z+z'-2L)} \right] \quad (87)$$

D. Transmission Line with Shunt-Current Source--Current-Source Green's Function

A zero-admittance point current source, $I_g(z')$, in shunt with the line at $z = z'$ is depicted in Figure 9. The boundary conditions at $z = z'$ and their relationships to transmission-line parameters in Regions 1 and 2

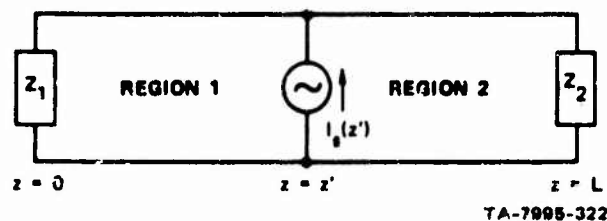


FIGURE 9 POINT SHUNT-CURRENT SOURCE

[Eqs. (73), (74), (79), and (80)] are given by

$$v_2^I(z') - v_1^I(z') = 0$$

$$= v_{2f}^I e^{-\gamma'} \left[1 + \rho_2 e^{2\gamma(z'-L)} \right] - v_1^I e^{\gamma z'} \left(1 + \rho_1 e^{-2\gamma z'} \right)$$

$$i_2^I(z') - i_1^I(z') = i_s(z')$$

$$= y_0 v_{2f}^I e^{-\gamma z'} \left[1 - \rho_2 e^{2\gamma(z'-L)} \right] + y_0 v_{1r}^I e^{\gamma z'} \left(1 - \rho_1 e^{-2\gamma z'} \right)$$

(88)

Solving for v_{1r}^I and v_{2f}^I gives

$$v_{1r}^I = \frac{z_0 i_s(z') e^{-\gamma z'} \left[1 + \rho_2 e^{2\gamma(z'-L)} \right]}{2 \left(1 - \rho_1 \rho_2 e^{-2\gamma L} \right)} \quad (89)$$

$$v_{2f}^I = \frac{z_0 i_s(z') e^{\gamma z'} \left(1 + \rho_1 e^{-2\gamma z'} \right)}{2 \left(1 - \rho_1 \rho_2 e^{-2\gamma L} \right)} \quad (90)$$

The Green's-function solution for Regions 1 and 2 is obtained by setting $I_s(z') = 1$ and substituting the expression for V_{1r}^I into Eqs. (73), (74), (79), and (80) for voltages and currents to give, in Region 1, where $z < z'$,

$$V_{1G}^I(z, z') = \frac{Z_0 \left[1 + \rho_2 e^{2\gamma(z'-L)} \right]}{2 \left(1 - \rho_1 \rho_2 e^{-2\gamma L} \right)} \left[e^{\gamma(z-z')} + \rho_1 e^{-\gamma(z+z')} \right] \quad (91)$$

$$I_{1G}^I(z, z') = - \frac{\left[1 + \rho_2 e^{-2\gamma(z'-L)} \right]}{2 \left(1 - \rho_1 \rho_2 e^{-2\gamma L} \right)} \left[e^{\gamma(z-z')} - \rho_1 e^{-\gamma(z+z')} \right] \quad (92)$$

and, in Region 2, where $z > z'$,

$$V_{2G}^I(z, z') = \frac{Z_0 \left(1 + \rho_1 e^{-2\gamma z'} \right)}{2 \left(1 - \rho_1 \rho_2 e^{-2\gamma L} \right)} \left[e^{-\gamma(z-z')} + \rho_2 e^{\gamma(z+z'-2L)} \right] \quad (93)$$

$$I_{2G}^I(z, z') = \frac{\left(1 + \rho_1 e^{-2\gamma z'} \right)}{2 \left(1 - \rho_1 \rho_2 e^{-2\gamma L} \right)} \left[e^{-\gamma(z-z')} - \rho_2 e^{\gamma(z+z'-2L)} \right] \quad (94)$$

E. Transmission Lines Terminated in Characteristic Impedance

In lines terminated in characteristic impedances,

$$\rho_1 = \rho_2 = 0 \quad (95)$$

and the Green's functions given by Eqs. (84) through (87) and (91) through (94) simplify to

$$\left. \begin{aligned} V_{1G}^V(z, z') &= -\frac{1}{2} e^{\gamma(z-z')} , & z < z' \\ I_{1G}^V(z, z') &= \frac{Y_0}{2} e^{\gamma(z-z')} , & z < z' \\ V_{2G}^V(z, z') &= \frac{1}{2} e^{-\gamma(z-z')} , & z > z' \\ I_{2G}^V(z, z') &= \frac{Y_0}{2} e^{-\gamma(z-z')} , & z > z' \end{aligned} \right\} \quad (96)$$

$$\left. \begin{aligned} V_{1G}^I(z, z') &= \frac{Z_0}{2} e^{\gamma(z-z')} , & z > z' \\ I_{1G}^I(z, z') &= -\frac{1}{2} e^{\gamma(z-z')} , & z < z' \\ V_{2G}^I(z, z') &= \frac{Z_0}{2} e^{-\gamma(z-z')} , & z > z' \\ I_{2G}^I(z, z') &= \frac{1}{2} e^{-\gamma(z-z')} , & z > z' \end{aligned} \right\} \quad (97)$$

The above Green's functions represent voltage or current propagated from the unit voltage or current source without reflection from the characteristic impedance terminations.

F. Coaxial-Cable Leakage

Analysis of leakage into a coaxial cable due to a uniformly distributed transfer impedance such as in braided exterior shields, and to localized leakage points from apertures at joints, cracks, and holes in the shield, is based on the discussion presented in previous sections. The coaxial cable is placed along the z -axis with one end terminated in impedance Z_1 at $z = 0$, and at the other end in impedance Z_2 at $z = L$.

To generalize the analysis slightly, the line is subdivided into N segments with $z_0 = 0 < z_1 < z_2 \dots < z_N = L$, and in the segment n , lying between z_{n-1} and z_n , there are N_n aperture leakage points. A line in which leakage occurs only in a segment from z_{n-1} to z_n is considered. A current $I'(z)$ is assumed to flow along the outside surface of the coaxial line. The zero-impedance voltage and zero-admittance current sources for small holes and joints in segment n is written as

$$V_{sp}(z) = \sum_{p=1}^{N_n} Z_p(z) \delta(z - z_{np}) I'(z) \quad (98)$$

$$I_{sp}(z) = \sum_{p=1}^{N_n} T_p(z) \delta(z - z_{np}) I'(z) \quad (99)$$

where z_{np} determines the location of the p^{th} aperture in segment n .

Distributed leakage impedance Z_D^* and transfer function T_D , describe the leakage properties of many perforations per unit length with each perforations treated as an aperture; but each unit length of line shows the same properties, so that Z_D and T_D are independent of z . The distributed zero-impedance voltage and zero-admittance current sources are expressed as

$$V_{sD}(z) = Z_D I'(z) \quad (100)$$

$$I_{sD}(z) = T_D I'(z) \quad (101)$$

between z_{n-1} and z_n . The composite sources then become

$$\begin{aligned} V_s(z) &= V_{sp}(z) + V_{sD}(z) \\ &= \left[\sum_{p=1}^{N_n} Z_p(z) \delta(z - z_{np}) + Z_D \right] I'(z) \end{aligned} \quad (102)$$

and

$$I_s(z) = \left[\sum_{p=1}^{N_n} T_p(z) \delta(z - z_{np}) + T_D \right] I'(z) \quad (103)$$

* Reference 4 gives an example of Z_D .

The voltages and currents along the line may be obtained by substituting $V_s(z)$ and $I_s(z)$ from Eqs. (102) and (103) into the superposition integral [Eqs. (57), (59), (60), and (61)]. The solutions have three forms, depending on whether the solution is in Region a_n where $z < z_{n-1}$, Region n where $z_{n-1} \leq z \leq z_n$, or Region b_n where $z > z_n$. The solutions are for Region a_n , where $z < z_{n-1}$,

$$V^V(z) = \sum_{p=1}^{N_n} Z_p(z_{np}) V_{1G}^V(z, z_{np}) I'(z_{np}) + Z_D \int_{z_{n-1}}^{z_n} I'(z') V_{1G}^V(z, z') dz' \quad (104)$$

$$I^V(z) = \sum_{p=1}^{N_n} Z_p(z_{np}) I_{1G}^V(z, z_{np}) I'(z_{np}) + Z_D \int_{z_{n-1}}^{z_n} I'(z') I_{1G}^V(z, z') dz' \quad (105)$$

$$V^I(z) = \sum_{p=1}^{N_n} T_p(z_{np}) V_{1G}^I(z, z_{np}) I'(z_{np}) + T_D \int_{z_{n-1}}^{z_n} I'(z') V_{1G}^I(z, z') dz' \quad (106)$$

$$I^I(z) = \sum_{p=1}^{N_n} T_p(z_{np}) I_{1G}^I(z, z_{np}) I'(z_{np}) + T_D \int_{z_{n-1}}^{z_n} I'(z') I_{1G}^I(z, z') dz' \quad (107)$$

For Region b_n , where $z > z_n$, equations are identical to those obtained for Region a_n except that the subscript 1 is changed to 2 so that V_{1G}^V , I_{1G}^V , V_{1G}^I , and I_{1G}^I become V_{2G}^V , I_{2G}^V , V_{2G}^I , and I_{2G}^I .

For Region n , where $z_{n-1} \leq z \leq z_n$,

$$V^V(z) = \sum_{p=p_z}^N Z_p(z_{np}) V_{1G}^V(z, z_{np}) I'(z_{np}) + Z_D \int_z^{z_n} I'(z') V_{1G}^V(z, z') dz' \quad (108)$$

$$+ \sum_{p=1}^{p_z-1} Z_p(z_{np}) V_{2G}^V(z, z_{np}) I'(z_{np}) + Z_D \int_{z_{n-1}}^z I'(z') V_{2G}^V(z, z') dz$$

$$V^I(z) = \sum_{p=p_z}^N T_p(z_{np}) V_{1G}^I(z, z_{np}) I'(z_{np}) + T_D \int_z^{z_n} I'(z') V_{1G}^I(z, z') dz' \quad (109)$$

$$+ \sum_{p=1}^{p_z-1} T_p(z_{np}) V_{2G}^I(z, z_{np}) I'(z_{np}) + T_D \int_{z_{n-1}}^z I'(z') V_{2G}^I(z, z') dz'$$

where p_z is the first leakage point in the segment between z and z_n .

The current expressions $I^V(z)$ and $I^I(z)$ are identical to the above

two equations with the replacement of V_{1G}^V , V_{2G}^V , V_{1G}^I , and V_{2G}^I by

I_{1G}^V , I_{2G}^V , I_{1G}^I , and I_{2G}^I . Since the voltage and current-source Green's

functions are the sum of two exponentials in z , the integrals in the

expression for voltages and currents are integrable for a large variety

of current functions, $I'(z)$.

G. Special Application

Sometimes it is useful to consider a very short segment of line from z_{n-1} to z_n with a current independent of z so that

$$I'(z) = I'_n. \quad (110)$$

Then the integral contributions to voltages and currents are just the integral of the Green's function. Evaluating the integrals of the Green's function gives the following relationships, where algebraic coincidence is the basis for equality between the second and third quantities:

$$\int V_{1G}^V(z, z') dz' = -\frac{1}{Y} \frac{1 + \rho_2 e^{2Y(z'-L)}}{1 - \rho_2 e^{2Y(z'-L)}} V_{1G}^V(z, z') = \frac{Y_0}{Y} V_{1G}^I(z, z') \quad (111)$$

$$\int I_{1G}^V(z, z') dz' = -\frac{1}{2} \frac{1 + \rho_2 e^{2Y(z'-L)}}{1 - \rho_2 e^{2Y(z'-L)}} I_{1G}^V(z, z') = \frac{Y_0}{Y} I_{1G}^I(z, z') \quad (112)$$

$$\int V_{2G}^V(z, z') dz' = \frac{1}{Y} \frac{1 + \rho_1 e^{-2Yz'}}{1 - \rho_1 e^{-2Yz'}} V_{2G}^V(z, z') = \frac{Y_0}{Y} V_{2G}^I(z, z') \quad (113)$$

$$\int I_{2G}^V(z, z') dz' = \frac{1}{Y} \frac{1 + \rho_1 e^{-2Yz'}}{1 - \rho_1 e^{-2Yz'}} I_{2G}^V(z, z') = \frac{Y_0}{Y} I_{2G}^I(z, z') \quad (114)$$

Similarly,

$$\int v_{1G}^I(z, z') dz' = -\frac{1}{\gamma} \frac{1 - \rho_2 e^{2\gamma(z'-L)}}{1 + \rho_2 e^{2\gamma(z'-L)}} v_{1G}^I(z, z') = \frac{z_0}{\gamma} v_{1G}^V(z, z') \quad (115)$$

$$\int i_{1G}^I(z, z') dz' = -\frac{1}{\gamma} \frac{1 - \rho_2 e^{2\gamma(z'-L)}}{1 + \rho_2 e^{2\gamma(z'-L)}} i_{1G}^I(z, z') = \frac{z_0}{\gamma} i_{1G}^V(z, z') \quad (116)$$

$$\int v_{2G}^I(z, z') dz' = \frac{1}{\gamma} \frac{1 - \rho_1 e^{-2\gamma z'}}{1 + \rho_1 e^{-2\gamma z'}} v_{2G}^I(z, z') = \frac{z_0}{\gamma} v_{2G}^V(z, z') \quad (117)$$

$$\int i_{2G}^I(z, z') dz' = \frac{1}{\gamma} \frac{1 - \rho_1 e^{-2\gamma z'}}{1 + \rho_1 e^{-2\gamma z'}} i_{2G}^I(z, z') = \frac{z_0}{\gamma} i_{2G}^V(z, z') \quad (118)$$

Substituting these results in the equation for voltages and currents in the three regions gives as typical examples for Region a_n where $z < z_{n-1}$,

$$v^V(z) = \left\{ \sum_{p=1}^{N_n} z_p(z_{np}) v_{1G}^V(z, z_{np}) + \frac{z_D y_0}{\gamma} [v_{1G}^I(z, z_n) - v_{1G}^I(z, z_{n-1})] \right\} I_n \quad (119)$$

and, for Region n, where $z_{n-1} < z < z_n$

$$V^V(z) \left\{ \sum_{p=p_z}^{N_n} z_p(z_{np}) V_{1G}^V(z, z_{np}) + \frac{z_D y_0}{\gamma} \left[V_{1G}^I(z, z_n) - V_{1G}^I(z, z) \right] \right. \\ \left. + \sum_{p=1}^{p=p_z-1} z_p(z_{np}) V_{2G}^V(z, z_{np}) + \frac{z_D y_0}{\gamma} \left[V_{2G}^I(z, z) - V_{2G}^I(z, z_{n-1}) \right] \right\} I_n \quad (120)$$

The equations occurring in Region n may be further simplified since

$$V_{1G}^I(z, z) = V_{2G}^I(z, z) \quad (121)$$

$$I_{1G}^V(z, z) = I_{2G}^V(z, z) \quad (122)$$

but

$$I_{1G}^I(z, z) \neq I_{2G}^I(z, z) \quad (123)$$

$$V_{1G}^V(z, z) \neq V_{2G}^V(z, z) \quad (124)$$

The solution, when one segment is the entire line, is obtained by setting $N = 1$. Then $z_{N-1} = z_0 = 0$ and $z_N = z_1 = L$.

H. Example of Leakage from Two Apertures

A simple example will illustrate the use of some of the results and their application to the interpretation of measurements. A lossless coaxial line of length L is terminated in its characteristic impedance $Z_0 = R_0$, at both ends of the line. The coaxial line has propagation constant $\gamma = \sqrt{ZY}$, where Z and Y are the distributed impedance and admittance per unit length. The line is subdivided into three segments by making divisions (see Figure 10), at $z = z_1$ and $z = z_2$ so that $N = 3$ and $z_3 = L$. As in Figure 10, two apertures are located in segment 2 at z_{21} and z_{22} , at a distance $d = z_{22} - z_{21}$ apart so that $z_1 < z_{21} < z_{22} < z_2$.

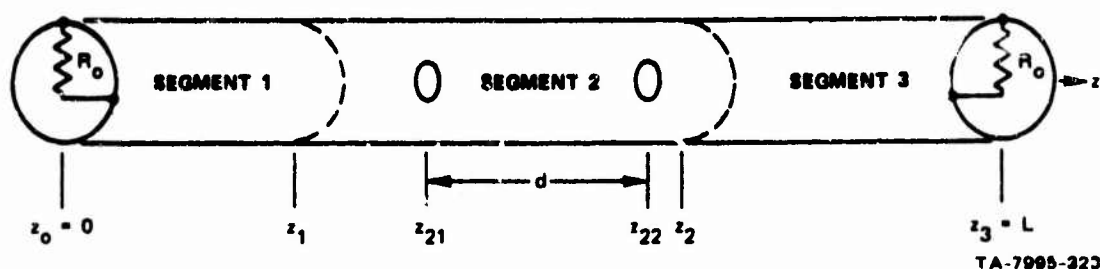


FIGURE 10 COAXIAL CABLE WITH TWO APERTURES

The transfer impedances and functions at the apertures are denoted by $Z_p(z_{21})$ and $T_p(z_{21})$ and by $Z_p(z_{22})$ and $T_p(z_{22})$.

A current, $I'(z) = I_1 e^{-\gamma' z}$, flows along the outer surface of the coaxial cable. The fields associated with this current leak into the coaxial cable through the apertures. Leakage voltages across R_0 terminating the coaxial cable are to be determined. The voltage at $z_0 = 0$ is determined from the sum of $V^V(z)$, given by Eq. (104), and $V^I(z)$, given by Eq. (106). The voltage at $z_3 = L$ is determined from the sum of $V^V(z)$ and $V^I(z)$, given by Eqs. (104) and (106), respectively, but the voltage- and current-source Green's functions are replaced by V_{2G}^V and V_{2G}^I as well as $z = L$ for region where $z > z_2$.

Substituting into Eqs. (104) and (106) with Green's functions given by the first expressions in Eqs. (96) and (97) yields the expression for voltage in Region $z < z_1$:

$$\begin{aligned} V^V(z) &= Z_p(z_{21}) \left[-\frac{1}{2} e^{\gamma(z-z_{21})} \right] I_0 e^{-\gamma' z_{21}} + Z_p(z_{22}) \left[-\frac{1}{2} e^{\gamma(z-z_{22})} \right] I_0 e^{-\gamma' z_{22}} \\ &= -\frac{1}{2} \left[Z_p(z_{21}) e^{-(\gamma+\gamma')z_{21}} + Z_p(z_{22}) e^{-(\gamma+\gamma')z_{22}} \right] I_0 e^{\gamma z} \quad (125) \end{aligned}$$

$$V^I(z) = \frac{1}{2} \left[T_p(z_{21}) e^{-(\gamma+\gamma')z_{21}} + Z_p(z_{22}) e^{-(\gamma+\gamma')z_{22}} \right] Z_0 I_0 e^{\gamma z} \quad (126)$$

Hence,

$$\begin{aligned} V(z) &= V^V(z) + V^I(z) \\ &= \frac{1}{2} \left\{ \left[Z_0 T_p(z_{21}) - Z_p(z_{21}) \right] e^{-(\gamma+\gamma')z_{21}} \right. \\ &\quad \left. + \left[Z_0 T_p(z_{22}) - Z_p(z_{22}) \right] e^{-(\gamma+\gamma')z_{22}} \right\} I_0 e^{\gamma z} \quad (127) \end{aligned}$$

For the region $z > z_2$, a similar development gives

$$V(z) = \frac{1}{2} \left\{ \left[Z_{0p}^T(z_{21}) + Z_p(z_{21}) \right] e^{(\gamma - \gamma') z_{21}} + \left[Z_{0p}^T(z_{22}) + Z_p(z_{22}) \right] e^{(\gamma - \gamma') z_{22}} \right\} I_0 e^{-\gamma z} \quad (128)$$

Since

$$z_{22} = z_{21} + d \quad (129)$$

Eqs. (127) and (128) become, for $z < z_1$,

$$V(z) = \frac{1}{z} \left\{ \left[Z_{0p}^T(z_{21}) - Z_p(z_{21}) \right] + \left[Z_{0p}^T(z_{22}) - Z_p(z_{22}) \right] e^{-(\gamma + \gamma') d} \right\} I_0 e^{\gamma z - (\gamma + \gamma') z_{21}} \quad (130)$$

and for $z > z_2$,

$$V(z) = \frac{1}{2} \left\{ \left[Z_{0p}^T(z_{21}) + Z_p(z_{21}) \right] + \left[Z_{0p}^T(z_{22}) + Z_p(z_{22}) \right] e^{(\gamma - \gamma') d} \right\} I_0 e^{-\gamma z + (\gamma - \gamma') z_{21}} \quad (131)$$

The implications of Eqs. (130) and (131) are clarified by considering a special case of identical apertures and $\gamma = \gamma' = j\omega/c$ for air dielectric both outside and inside a lossless coaxial line. Also, the aperture is assumed to be described by one component of the magnetic-dipole moment as in circular apertures or where the magnetic field is predominantly along one of the orthogonal magnetic-polarizability axes. Substituting the transfer-impedance and function expressions from Eqs. (20) and (30), the leakage-voltage expressions at the ends of the coaxial line become, for $z < z_1$,

$$V(z) = - \frac{j\omega\mu_0 Me}{8\pi^2 R'^2} \left(1 - \frac{Pe}{Me} \frac{-\gamma_E^T}{-\gamma_H^T} \right) \left(1 + e^{-2\gamma d} \right) I_0 e^{\gamma z - 2\gamma z_{21}} \quad (132)$$

and for $z > z_2$,

$$V(z) = \frac{j\omega\mu_0 Me}{4\pi^2 R'^2} \left(1 + \frac{Pe}{Me} \frac{-\gamma_E^T}{-\gamma_H^T} \right) I_0 e^{-\gamma z} \quad (133)$$

The polarity of $V(z)$ is such that the center conductor of the coaxial line is at a lower potential than the outer conductor.

Since $\gamma d = j\omega d/c$ and both γ_E and γ_H are real, the ratio of measured voltage at the end of the coaxial cable to the current flowing on the outside of the coaxial cable is, for $z < z_1$,

$$\frac{|V|}{|I_0|} = \frac{\omega\mu_0 Me}{\sqrt{2} 4\pi^2 R'^2} \left| 1 - \frac{Pe}{Me} \frac{-\gamma_E^T}{-\gamma_H^T} \right| \sqrt{1 + \cos \frac{2\omega d}{c}} \quad (134)$$

and for $z > z_2$,

$$\frac{|V|}{|I_0|} = \frac{\frac{\mu Me}{4\pi^2 R'^2} \frac{-\gamma_H^T}{H}}{1 + \frac{Pe}{Me} \frac{\frac{-\gamma_E^T}{E}}{\frac{-\gamma_H^T}{H}}} \quad (135)$$

Letting

$$D = \frac{Pe}{Me} \frac{\frac{-\gamma_E^T}{E}}{\frac{-\gamma_H^T}{H}} \quad (136)$$

the leakage behavior of the two identical apertures, from Eqs. (134) and (135), can be written for $z < z_1$ as

$$\begin{aligned} \left| \frac{V}{I} \right|_{dB} = & 20 \log \frac{\frac{\mu Me}{4\pi^2 R'^2} \frac{-\gamma_H^T}{H}}{1 - D} + 20 \log |1 - D| + 20 \log f_{MHz} \\ & + 10 \log \left(1 + \cos \frac{\pi}{75} df_{MHz} \right) + 133 \end{aligned} \quad (137)$$

and for $z > z_2$ as

$$\left| \frac{V}{I} \right|_{dB} = 20 \log \frac{\frac{\mu Me}{4\pi^2 R'^2} \frac{-\gamma_H^T}{H}}{1 + D} + 20 \log |1 + D| + 20 \log f_{MHz} + 136 \quad (138)$$

where

$$f_{\text{MHz}} = \text{frequency in MHz}$$

and

$$D = \frac{P_e}{P_m} \frac{-\gamma_E^T}{-\gamma_H^T} \quad (139)$$

The relative coupling to $z < z_1$ and $z > z_2$ is

$$C_R = \left| \frac{V_{z < z_1}}{V_{z > z_2}} \right|_{\text{dB}} = \left| \frac{I_{z < z_1}}{I_{z > z_2}} \right| = 20 \log |1 - D|$$

$$+ 10 \log \left(1 + \cos \frac{\pi}{75} df_{\text{MHz}} \right) - 20 \log |1 + D| - 3 \quad (140)$$

where the voltage and current ratios are identical because of characteristic resistance terminations.

A circular hole in an infinite thin outer conductor has a value for D given by

$$D = \frac{P}{M} = \frac{\frac{2}{3}r^3}{\frac{4}{3}r^3} = \frac{1}{2} \quad (141)$$

The relative coupling to both sides of the holes then becomes

$$C_R = 10 \log \left(1 + \cos \frac{\pi}{75} df_{\text{MHz}} \right) - 9.52 \quad (142)$$

With two circular holes of radius 10^{-4} m separated by a distance, $d = 3$ m, and a radius of 10^{-2} m for the outer conductor of air-filled coaxial line, the coupled leakage becomes, for $z < z_1$,

$$\left| \frac{V}{I} \right|_{\text{dB}} = 20 \log f_{\text{MHz}} + 10 \log \left(1 + \cos \frac{3\pi}{75} f_{\text{MHz}} \right) - 217.44 \quad (143)$$

and for $z > z_2$,

$$\left| \frac{V}{I} \right|_{\text{dB}} = 20 \log f_{\text{MHz}} - 207.92 \quad (144)$$

Equation (142) is plotted in Figure 11 for the case of $d = 3$ m, together with the case of single-hole coupling. The absolute coupling expressed by Eqs. (143) and (144) is plotted in Figure 12 together with the case of single-hole coupling. The nulling effects are caused by equal coupling through both holes and would not happen if the hole sizes were different.

The absolute coupling as indicated in Figure 12 is large since the coupling apertures were in an infinitely thin outer shield of the coaxial line. If the outer shield were 10^{-3} m thick, the attenuation factor for electric polarizability would be 9.03×10^{-2} and for the magnetic polarization would be 1.586×10^{-1} , so that D would be equal to 0.294. Then the relative coupling to both ends of the line would be decreased by -2.45 dB. Also the absolute coupling for $z < z_1$ is decreased by about 18.9 dB and for $z > z_2$ by about 13.8 dB. The attenuation factors are functions of frequency, but for these frequencies and aperture size, the factors may be considered to be constants.

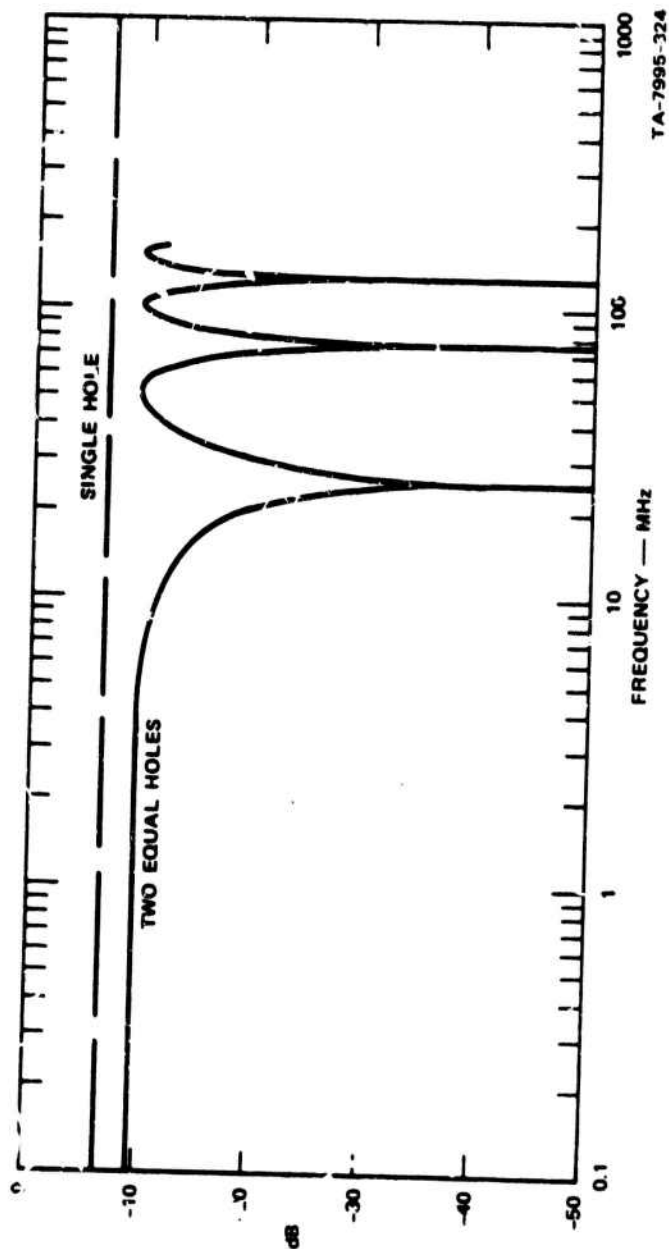
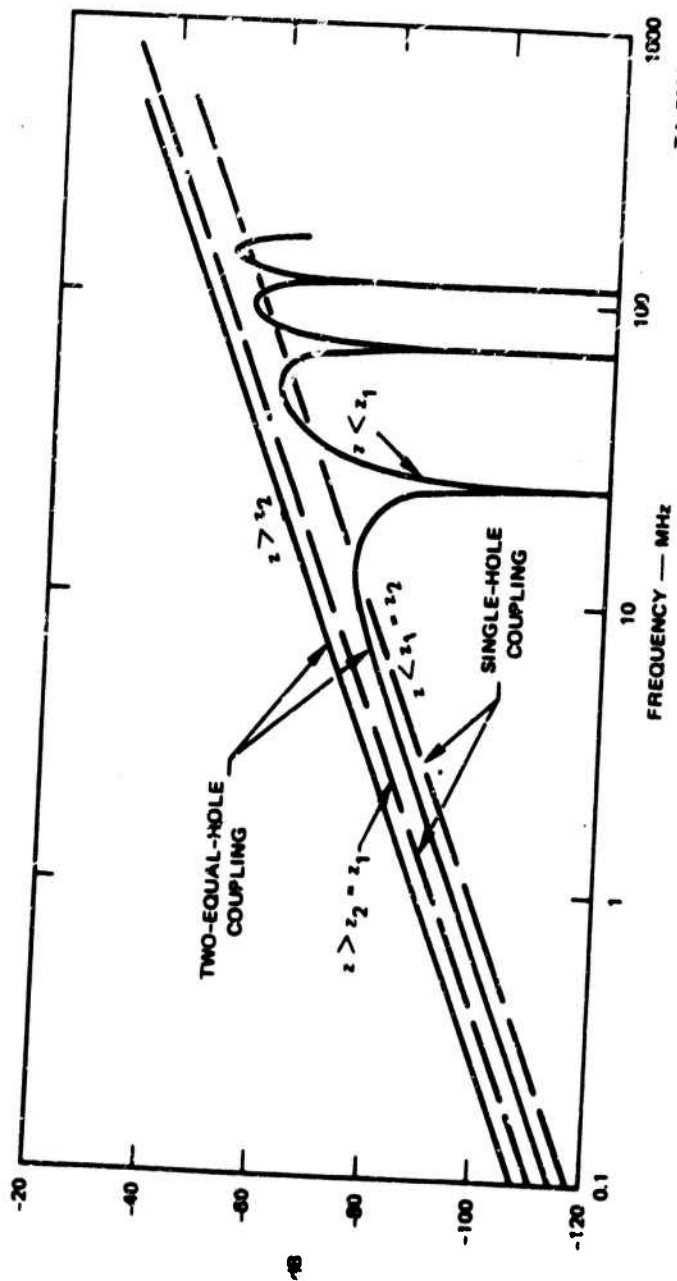


FIGURE 11 RELATIVE COUPLING OF TWO HOLES IN A COAXIAL LINE
WITH AN INFINITELY THIN CONDUCTOR



TA-7595-325

FIGURE 12 COUPLING THROUGH CIRCULAR HOLES IN AN INFINITELY THIN OUTER CONDUCTOR OF AN AIR COAXIAL LINE

IV CONCLUSIONS

Leakage on a shielded-cable system has been treated by assuming a current flowing on the exterior surface of a coaxial line. Voltage and current source that depends on leakage through an aperture in the exterior shield is developed to excite the coaxial line. Voltage and current expressions along the coaxial line, terminated in arbitrary impedances, are derived.

Aperture polarizabilities are considered to be empirical constants in the derivation, since the dimensions of apertures are impossible to determine. Values of polarizabilities are listed in Table 1 to illustrate the general relationships of aperture dimensions to polarizabilities and to the relative magnitudes of magnetic and electric polarizabilities, so as to assist in evaluating measured results.

As mentioned in the introduction, the method of leakage measurement used on this work order was influenced by this analysis. The measurements are taken by allowing current to flow only across one connector, joint, or seam, by connecting a current source across such a junction. Leakage will be observed at the ends of the cable terminals. Such a measurement procedure is consistent with the analytical expressions that have been presented. It should be noted that driving the coaxial line and observing aperture leakage along the exterior of the shield has not been discussed, since exterior measurement of leakage from an aperture requires a knowledge of the near-zone radiation field of the aperture and the interaction of the measuring probe with this field.

Measurement on a cable system consisting of a shield enclosing a number of separate insulated conductors will not give the same result as for the single concentric coaxial cable, which was analyzed, since the equivalent leakage voltage and current sources to each of the conductors would be different. An analysis based on multiconductor transmission line⁵ would also be required. Hence, allowance for differences between analysis and measurements should be considered in evaluating shielded cable systems. Nevertheless, the difficulty in describing leaky apertures and the simpler analysis and interpretation possible for a coaxial cable justifies the present approach for evaluating cable leakage effects.

REFERENCES

1. C. G. Montgomery, R. H. Dicke, and E. M. Purcell, "Principles of Microwave Circuits," MIT Rad. Lab. Series, Vol. 8 (McGraw-Hill Book Company, Inc., New York, N.Y., 1948).
2. N. Mercuvitz, Waveguide Handbook, MIT Rad. Lab. Series, Vol. 10 (McGraw-Hill Book Company, New York, N.Y., 1951).
3. W. L. Weeks, Electromagnetic Theory for Engineering Applications (John Wiley & Sons, Inc., New York, N.Y., 1964).
4. E. F. Vance, and H. Chang, "Shielding Effectiveness of Braided-Wire Shields," Technical Memorandum 18, Contract SRI Project 7995, Stanford Research Institute, Menlo Park, Calif. (November 1971).
5. S. Dairiki, and E. F. Vance, "Analysis of Commercial Power Line System," Technical Report, SRI Project 7995, Stanford Research Institute, Menlo Park, Calif. (to be published).